JOURNAL OF GEOPHYSICAL RESEARCH, VOL. 106, NO. D13, PAGES 14,235–14,243, JULY 16, 2001

The effect of precipitation variability on ENSO/precipitation teleconnections in the contiguous United States

A. A. Tsonis
Department of Mathematical Sciences, Atmospheric Sciences Group, University of Wisconsin-Milwaukee, Milwaukee, Wisconsin

C. C. Young-Molling
Space Science and Engineering Center, University of Wisconsin-Madison, Madison, Wisconsin

Abstract. An investigation of the spatiotemporal tendencies of the parameters of the probability density function describing precipitation in the last century in the contiguous United States reveals the existence of statistically significant local trends in both space and time. In such a case the distribution describing precipitation at a site is not constant in time, meaning that the population characteristics have not remained the same throughout the century. Here we show that when this variability is taken into account, it alters the effect of El Niño-Southern Oscillation (ENSO) on precipitation significantly and may often lead to erroneous predictions of ENSO-related precipitation patterns.

1. Introduction

One of the most important issues facing atmospheric sciences today is the El Niño-Southern Oscillation (ENSO) cycle and its effects on climate. ENSO refers to the irregularly occurring cycle of warm and cool water in the equatorial eastern and central Pacific Ocean. This warming and cooling cycle interacts with the atmosphere, thus affecting the atmospheric general circulation. Changes in the general circulation result in changes in regional precipitation patterns. It is reasonable then to assume that ENSO-precipitation teleconnections may exist. In the context of climate, teleconnections are correlations between variables in one region with variables in another (correlations here do not necessarily suggest linearity). Several studies in the past have indeed suggested that precipitation variability in the contiguous United States is strongly linked to the ENSO cycle [*Gershunov* and *Barnett*, 1988a, 1998b; *Ropelewski* and *Halpert*, 1996; *Trenberth et al.*, 1998]. For example, during El Niño events the southeastern United States and California receive above average precipitation amounts, while the northwestern United States receives below average amounts. During La Niña events the picture is approximately reversed. In a recent study [*Gershunov et al.*, 1999] it was suggested that El Niño/precipitation teleconnections over the United States are stronger during high phases of the North Pacific Oscillation (NPO) and weaker during low NPO phases. This study indicated that other factors may influence the effect of ENSO on precipitation, some of which might be explained by the nonlinear response of the atmospheric circulation to ENSO events. The existence and details of such teleconnections are important because if they are not taken into account, they could stand as a source of significant error for long-term forecasts based on ENSO phenomena.

While various approaches for revealing ENSO/precipitation teleconnections have been proposed, a common parametric procedure is as follows. First, only El Niño years and the corresponding precipitation amounts are considered at a site. Then, the probability density function is estimated or the data are fit to a gamma distribution. This distribution is assumed to represent the precipitation population for El Niño years. The same is repeated for only La Niña years, resulting in another distribution representing the precipitation population for La Niña years. Having these distributions, one can then compare certain statistics such as the median (or other percentiles), mean, variance, etc. Since El Niño and La Niña events are "scattered" in time, this approach is sound only if the parameters of the El Niño or La Niña precipitation population remain unchanged in time. Below we will show that this assumption is often violated, and as such one is sampling from mixed distributions. This, if not taken into account, may introduce significant errors in the statistics relevant to ENSO/precipitation teleconnections.

Paper number 2000JD900626.
0148-0227/01/2000JD900626$09.00

2. Data Analysis and Results

We considered the comprehensive precipitation data set for global land area [*Bradley et al.*, 1987; *Diaz et al.*, 1989] which includes monthly precipitation amounts from several thousand stations from the mid 1800s to the late 1980s. Most of the records are not continuous in time, and the number of stations has varied. Then we considered the contiguous United States and found which stations have uninterrupted monthly values for a period of 90 years. The optimum 90-year interval (the one that includes the latest years and results in a good number of suitable stations) is 1900-1989 (151 stations). These steps eliminate problems with missing data and at the same time provide a large enough sample to perform a rigorous analysis. The area and stations considered are shown in Figure 1. Subsequently, for each station we considered the first 40-year period, produced seasonal (December-January-February (DJF)) values, and from these 40 values estimated the likelihood estimates of the parameters of the gamma distribution. DJF values were chosen because this season is associated with the strongest ENSO response in the United States. The gamma distribution fits precipitation data very well [*Karl et al.*, 1995; *Bradley et al.*, 1987; *Ropelewski and Jalickee*, 1984] and allows the detection of changes in the precipitation field by monitoring changes in the parameters of the distribution.

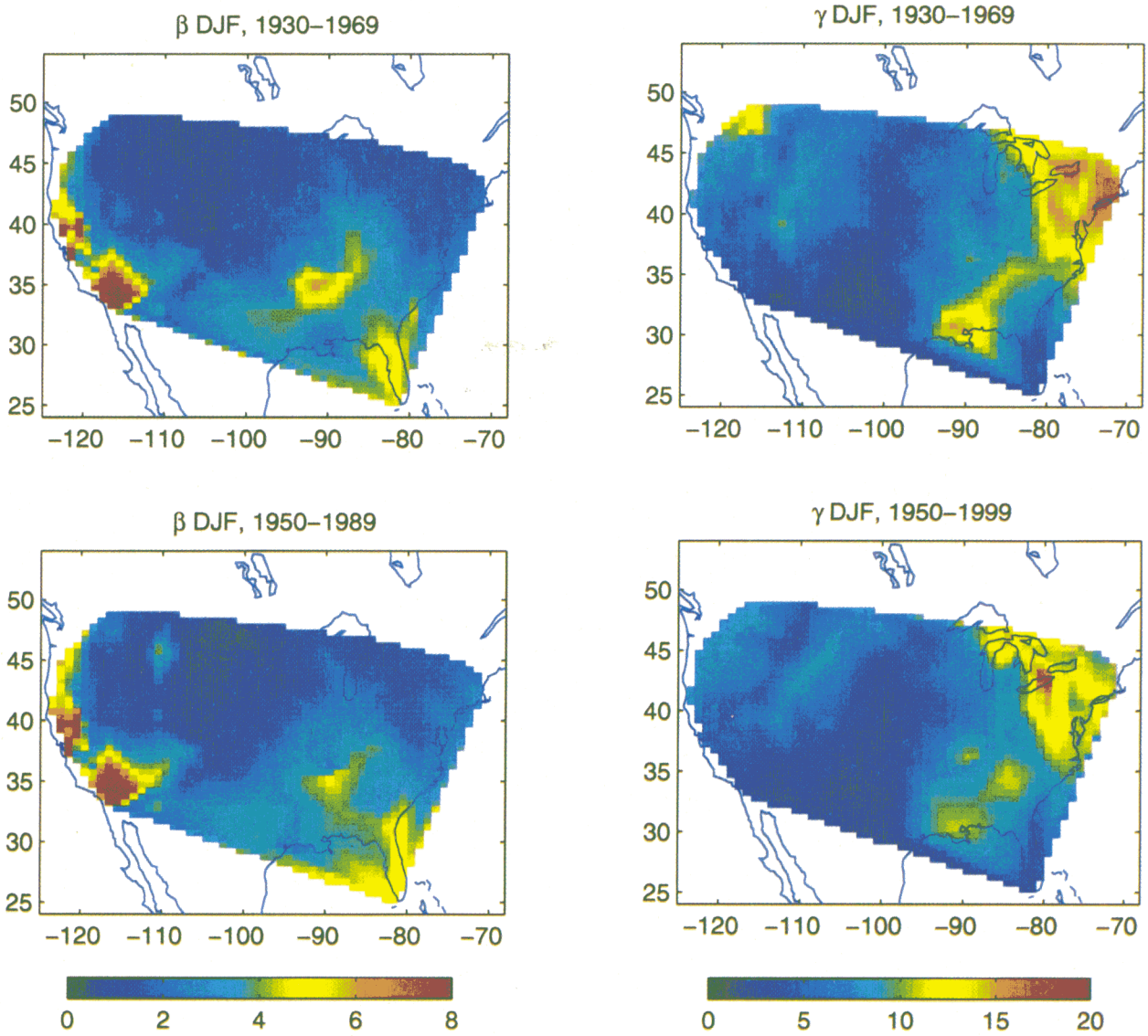

Plate 1. Examples of spatial distribution of the parameters (left) $\widehat{\beta}$ and (right) $\widehat{\gamma}$ of the gamma distribution in the United States for two selected 40-years period. According to the formulation of $\widehat{\beta}$ and $\widehat{\gamma}$, the units of $\widehat{\beta}$ are the same as the quantity we are measuring (centimeters), while $\widehat{\gamma}$ is dimensionless. The apparent overall "shift" of the plot eastward is an artifact of the interpolating scheme. See text for more details.

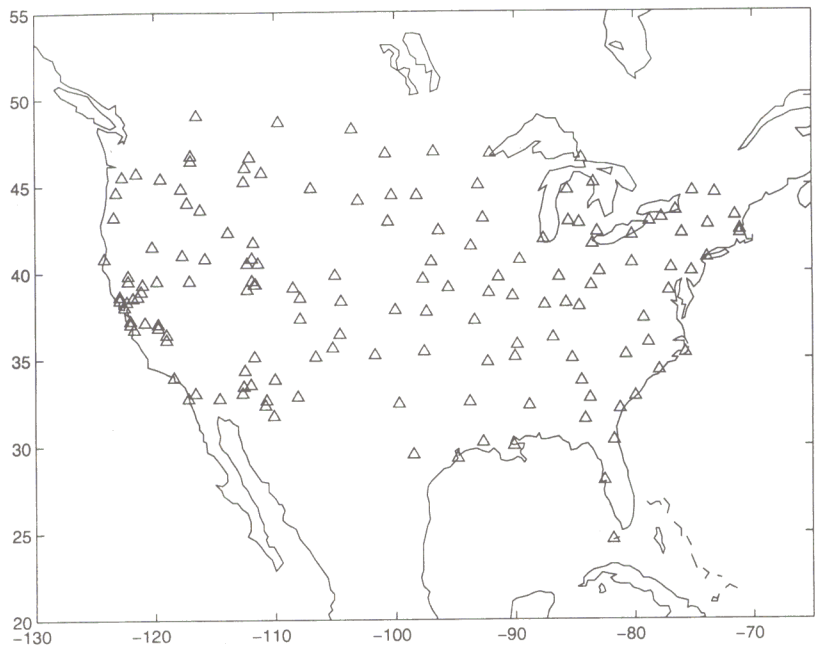

Figure 1. Areas and stations used in this study. All stations in these areas have uninterrupted monthly precipitation values for 90 years.

The advantage of modeling with the gamma distribution, as opposed to using the observed distribution, is that the gamma distribution can be used to analytically estimate the effect of changes in its parameters on the estimation of statistics such as the mean, median, or other percentiles. The gamma distribution is given by $f(x) = \beta^{-\gamma} x^{\gamma-1} e^{-(x/\beta)}/\Gamma(\gamma)$ $(\beta > 0, \gamma > 0)$, where x is the random value, Γ is the gamma function, and β and γ are the scale and shape parameters, respectively. The approximate maximum likelihood estimates for β and γ from a sample of N measurements are given by $\widehat{\gamma} = [1 + (1 + 4A/3)^{1/2}]/4A$ and $\widehat{\beta} = \overline{x}/\widehat{\gamma}$, where $A = \ln \overline{x} - (\sum \ln x)/N$, and $\overline{x}$ is the sample mean [*Thom*, 1958]. An estimate of the mean and variance is given by $\widehat{\beta}\widehat{\gamma}$ and $\widehat{\beta}^2\widehat{\gamma}$, respectively. As explained in the work of *Tsonis* [1996], the error in $\widehat{\beta}$ or $\widehat{\gamma}$ for sample sizes greater than $N = 30$ is small. We should point out at this point that the estimates of β and γ are subject to uncertainty especially in dry regions with a large number of nonzero events. In such regions one large event can affect the estimation of β and/or γ. However, we find that overall there is very good agreement between the estimated and measured mean and variance of the precipitation field (see Plates 1 and 2 below).

Having $\widehat{\beta}$ and $\widehat{\gamma}$ for each station in the first 40-year interval, we could then produce a map reflecting the spatial distribution of $\widehat{\beta}$ and $\widehat{\gamma}$ in the selected areas. Then we shifted the 40-year interval by 5 years and repeated the above procedure until we reached the last available 40-year interval. Plate 1 shows the spatial distribution of $\widehat{\beta}$ and $\widehat{\gamma}$ for two selected 40-year periods. For comparison, Plate 2 shows the measured mean precipitation and variance in the same periods. The agreement between modeled and measured precipitation statistics is quite good even in dry areas such as in the southwestern and western United States. Having maps like Plate 1, one can produce maps that show the spatial distribution of the difference in $\widehat{\beta}$ and $\widehat{\gamma}$ between selected 40-year periods. These "tendency" maps delineate the spatiotemporal changes in $\widehat{\beta}$ and $\widehat{\gamma}$ and provide insights about the evolution of these parameters. An example of such maps is given in Plate 3. From Plate 3 it is clear that (1) local trends of the order of $\pm$ 1.5 cm/10 years and $\pm$ 5/10 years are present for $\widehat{\beta}$ and $\widehat{\gamma}$, respectively, and (2) these trends are not uniform or consistent in either time or space. Considering that the mean DJF precipitation (see Plate 2) varies from 0 to 40 cm, such trends would correspond to changes in the mean of 20% or more at many locations. Nevertheless, in order to assess whether these trends are statistically significant and are not the result of sampling differences, we adapted the following Monte Carlo procedure. First, we consider a site and two 40-year periods. Let us assume that the two 40-year periods have $\widehat{\beta}_1, \widehat{\gamma}_1$ and $\widehat{\beta}_2, \widehat{\gamma}_2$ and that they overlap by M years. This defines a $\Delta\widehat{\beta}$ and a $\Delta\widehat{\gamma}$. Then we considered the second 40-year interval; we removed the 40-M nonoverlapping years and selected at random 40-M values from the gamma distribution describing the first 40-year period. This results in a new set of $\widehat{\beta}_2$ and $\widehat{\gamma}_2$ and thus in a new set of $\Delta\widehat{\beta}$ and $\Delta\widehat{\gamma}$. By repeating this procedure 1000 times, we can then estimate the probability distributions for $\Delta\widehat{\beta}$ and $\Delta\widehat{\gamma}$. If, for a given significance level α, the difference between $\widehat{\beta}_1$ and $\widehat{\beta}_2$ and/or $\widehat{\gamma}_1$ and $\widehat{\gamma}_2$ is due to

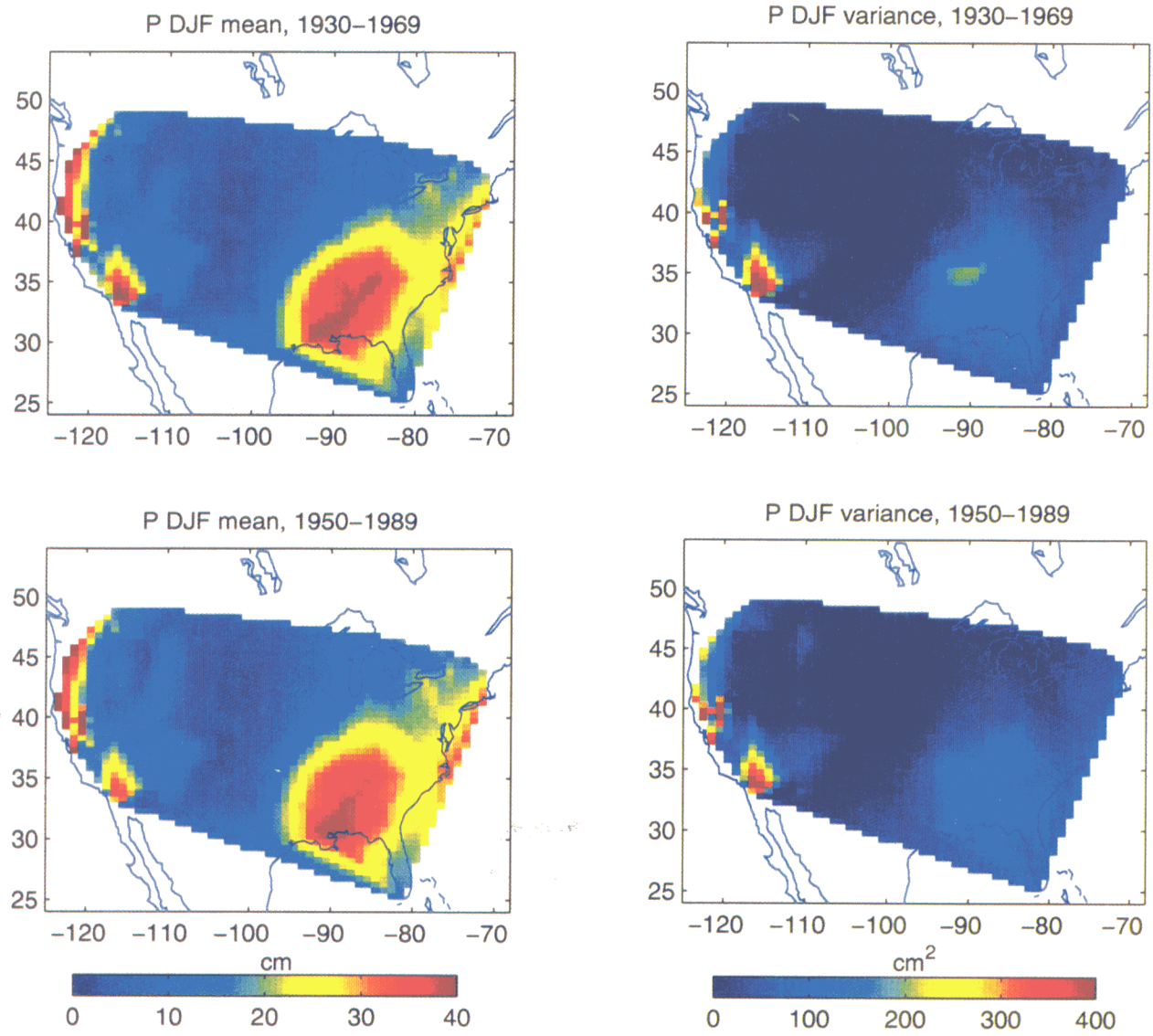

Plate 2. Spatial distribution of the (left) mean and (right) variance of the measured DJF precipitation amount for the 40-year periods of Plate 1. Comparison between Plates 1 and 2 indicates that the agreement between measured and modeled mean and variance ($\widehat{\beta\gamma}$ and $\widehat{\beta^2\gamma}$, respectively) is very good.

sampling differences, then the estimate from the two 40-year intervals $\Delta\widehat{\beta}$ and/or $\Delta\widehat{\gamma}$ will lie within the confidence interval $1-\alpha$, i.e., in the region where the null hypothesis $\Delta\widehat{\beta}=0$ or $\Delta\widehat{\gamma}=0$ is accepted. Otherwise it lies in the critical region where the null hypothesis is rejected. With this arrangement it is clear that for a site there is a $100\alpha\%$ probability that a significant trend in either parameters will occur simply by change. For the examples in Plate 3, Plate 4 shows the areas where local trends are statistically significant at the significance level $\alpha=0.1$. We find that, depending on the 40-year periods, up to 50% of the area may be experiencing a significant trend in either or both parameters. We also find that as the level of significance increases, the "significant" areas decrease but the main features remain the same. From the results presented up to now, we conclude that the observed variability in Plate 3 is a reflection of the complexity of precipitation rather than a result of sampling differences.

In order to now tie these facts back to ENSO, we considered the period 1900-1989 and found 40 El Niño years and 40 La Niña years. These years were determined from the NINO3 sea surface temperature (SST) data. The years corresponding to the 40 highest positive yearly SST values were included in the El Niño years set, and the years corresponding to the 40 lowest negative yearly SST values were included in the La Niña years set. From the yearly precipitation amounts in those years, we first generated for each set a figure similar to Plate 1. Then we calculated the difference in

$\widehat{\beta}$ and $\widehat{\gamma}$ between the set and selected 40-year periods. For the El Niño set the results are shown in Plate 5 and for the La Niña set, in Plate 6. By employing the results reported above we can clearly see that significant differences in $\widehat{\beta}$ and $\widehat{\gamma}$ are observed in many places. In fact, comparison between Plates 3, 5, and 6 shows that the differences are now more pronounced as higher $|\Delta\widehat{\beta}|$ and $|\Delta\widehat{\gamma}|$ are observed in Plates 5 and 6 than in Plate 3. An interesting observation in Plates 5 and 6 is that it appears that the details in Plate 5 are opposite to those in Plate 6. In Plate 5 the overall tendency is for negative $\Delta\widehat{\beta}$ and positive $\Delta\widehat{\gamma}$, while in Plate 6 the tendency is for positive $\Delta\widehat{\beta}$ and negative $\Delta\widehat{\gamma}$. The question then arises: How do these trends in the parameters of the gamma distribution affect the strength of ENSO-precipitation teleconnections? An answer to this question is provided next.

Given the gamma distribution, we have that the probability that a random variable x will take on a value less than or equal to X is $P_{\beta,\gamma}(x \leq X) = 1/\Gamma(\gamma)\ \beta^{-\gamma} \int_0^X x^{\gamma-1}\ e^{-x/\beta} dx$. By evaluating this integral for a fixed X, we can estimate $P(x \leq X)$ as a function of β and γ. Figure 2 shows this probability for $X = 25$ cm. Combining Figure 2 with Plates 1, 3, 5, and 6, one can observe that in areas like California and the southwestern United States (where $5 < \widehat{\beta} < 8, 0 < \widehat{\gamma} < 6$) or the Gulf of Mexico states and the southeastern United States (where

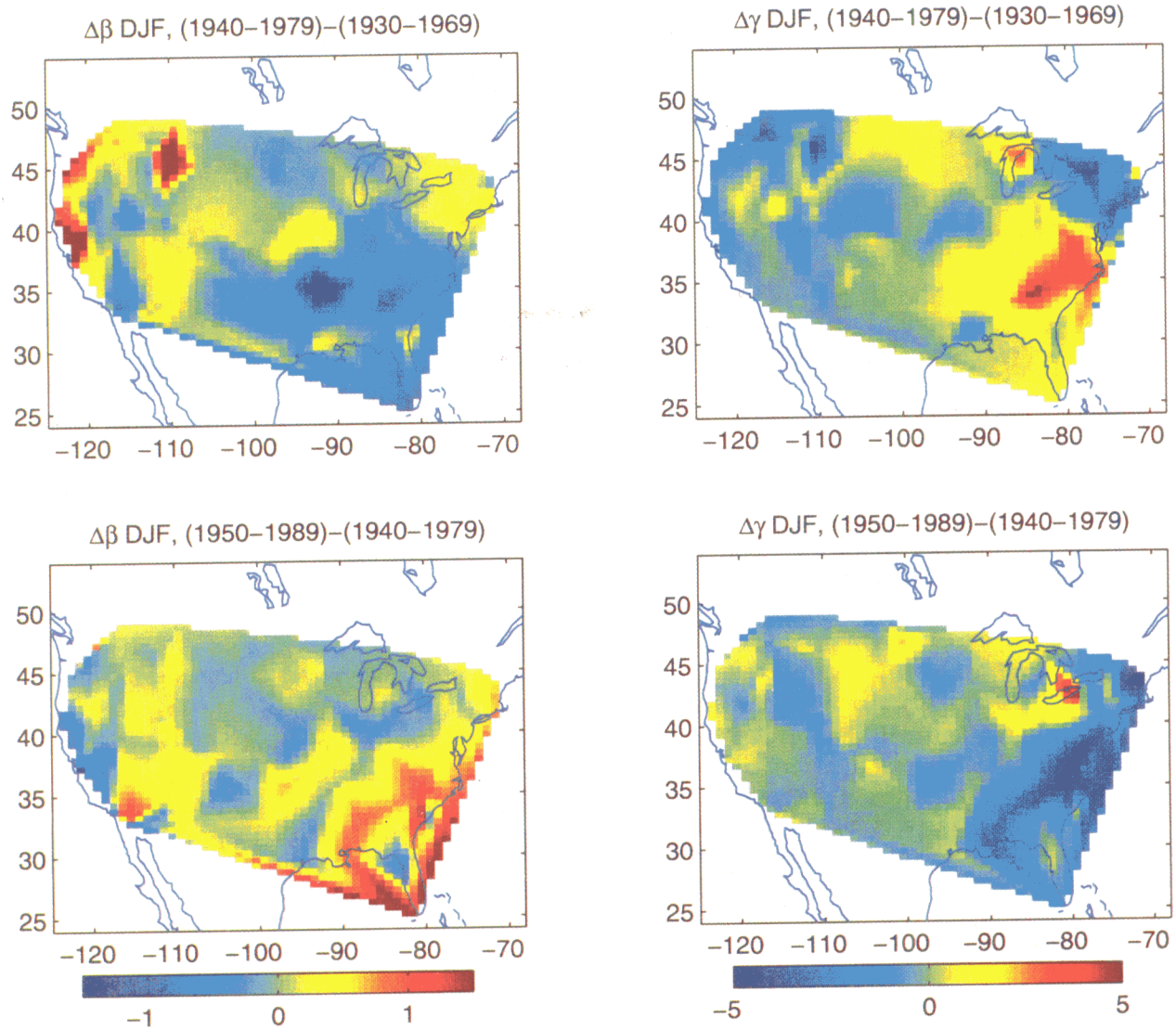

Plate 3. Examples of the spatial distribution of the difference in (left) $\widehat{\beta}$ and (right) $\widehat{\gamma}$ in the United States between selected 40-year periods. These "tendency" maps delineate the spatiotemporal changes in $\widehat{\beta}$ and $\widehat{\gamma}$ and can help provide information about the evolution of these parameters.

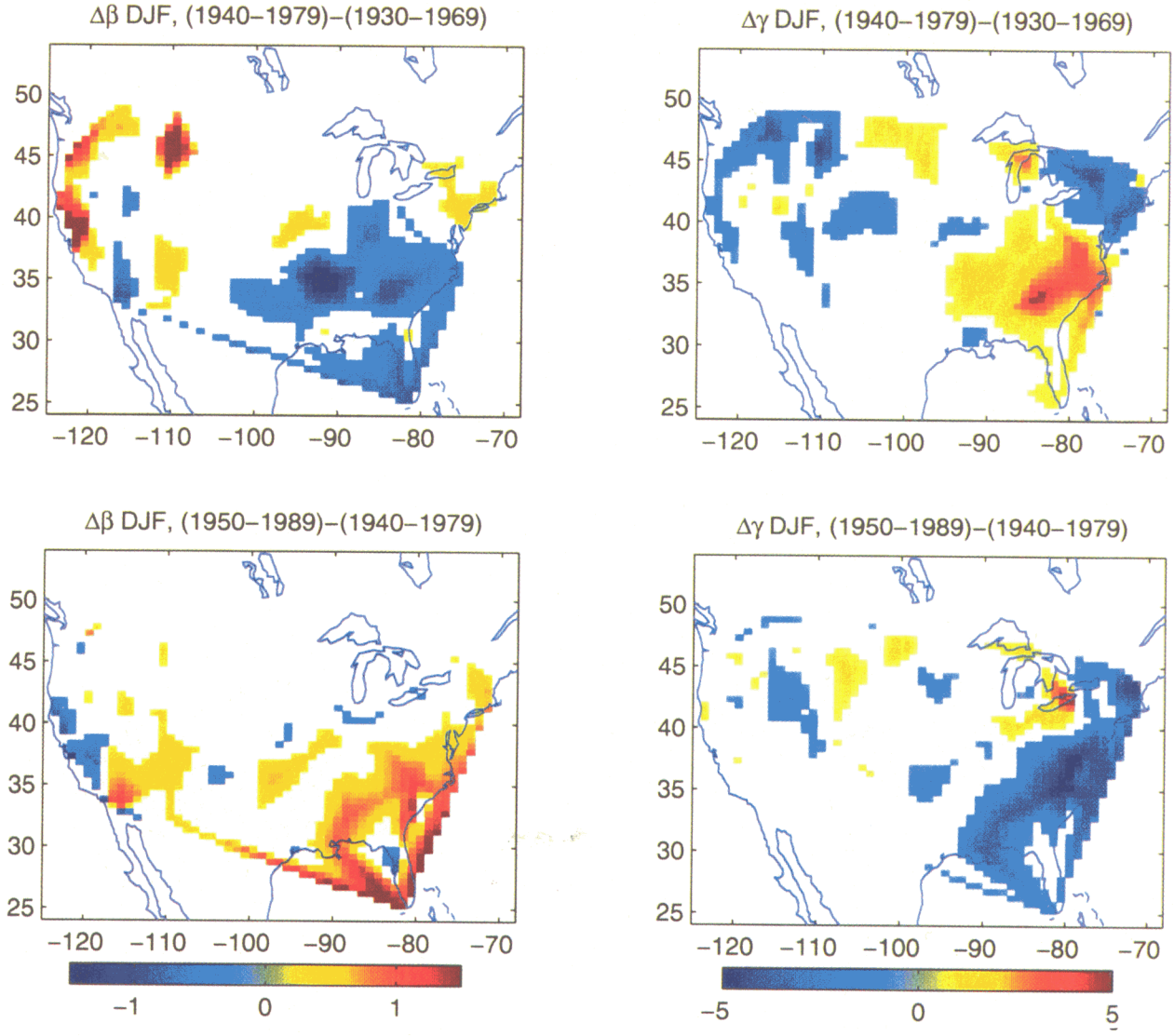

Plate 4. Areas for which the reported trends in Plate 2 are statistically significant at the 0.1 significance level. See text for details.

$3 < \widehat{\beta} < 6, 5 < \widehat{\gamma} < 15$) or the northeastern United States (where $\widehat{\beta} < 3, \widehat{\gamma} > 10$), significant fluctuations in $P(x \leq X)$ occur even for small changes in $\widehat{\beta}$ and/or $\widehat{\gamma}$. For example, for a site in the southeastern United States with $\widehat{\beta} = 4$ and $\widehat{\gamma} = 8$, a moderate change in $\widehat{\beta}$ by +0.5 and in $\widehat{\gamma}$ by +1.0 results in a change in $P(x \leq X)$ from 0.3 to 0.1. For a site in the northeastern United States with $\widehat{\beta} = 1.5$ and $\widehat{\gamma} = 15$, a similar change in $\widehat{\beta}$ and $\widehat{\gamma}$ results in a change in $P(x \leq X)$ from 0.7 to 0.2. For a site in California or the southwestern United States with $\widehat{\beta} = 7$ and $\widehat{\gamma} = 5$ it results in a change in $P(x \leq X)$ from 0.3 tp 0.13. Even larger changes in $P(x \leq X)$ are observed over these areas for greater changes in $\widehat{\beta}$ and/or $\widehat{\gamma}$. As such, in these areas as $\widehat{\beta}$ and $\widehat{\gamma}$ fluctuate in time, the median and other percentiles will be affected significantly (either increase or decrease depending on whether or not ΔP decreases or increases). This has the effect of increasing the uncertainty of the El Niño and La Niña effect on precipitation in these regions. This, if not taken into account, may lead to erroneous predictions of ENSO-related precipitation patterns. Note that in these regions mean DJF precipitation amounts (see Plate 2) range from about 20 cm to about 40 cm. As such, the choice of a threshold $X = 25$ cm is an appropriate one. In the central and northwestern United States, where $\widehat{\beta} < 2$ and $\widehat{\gamma} < 8$, and according to Plate 5, no significant changes in $P(x \leq X)$ are observed. This is due to the fact that in these areas the mean DJF precipitation amounts hardly exceed 10 cm, and therefore the choice of $X = 25$ is not appropriate. For appropriate thresholds, similar differences are observed there as well.

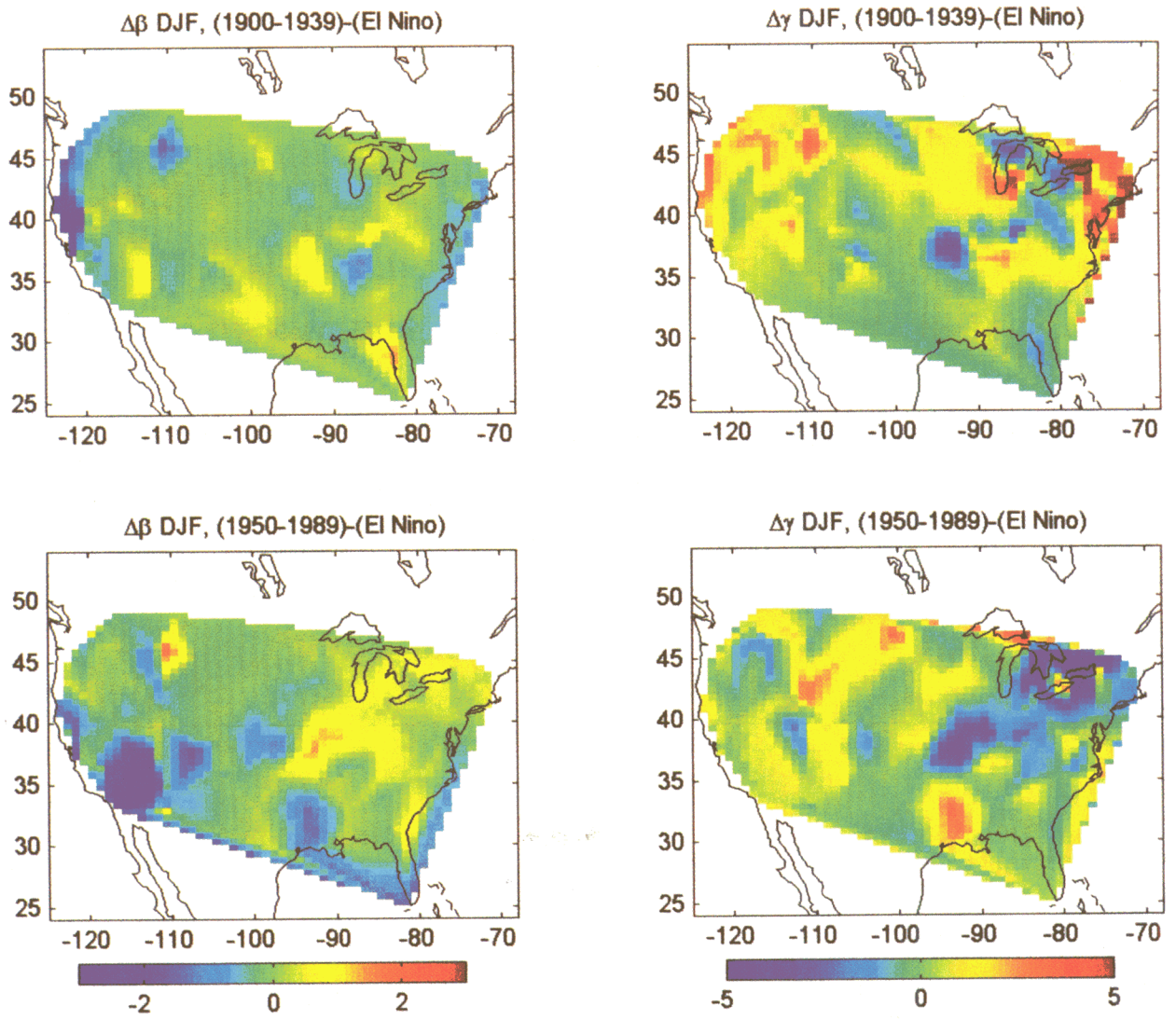

Plate 5. Same as Plate 3, but here the difference in (left) $\widehat{\beta}$ and (right) $\widehat{\gamma}$ is between selected 40-year intervals and the El Niño data set.

3. Concluding Remarks

From the above results it is clear that the precipitation population characteristics exhibit great spatiotemporal fluctuations. Thus a sample that includes years that are not successive in time will include values that come from different distributions. The estimated probability density function from this sample cannot account for the evolution of the actual probability density function of precipitation. This introduces an uncertainty in the estimation of a given percentile, and as such its net effect is to increase the sensitivity of ENSO/precipitation teleconnections. This may explain why models often fail to predict the El Niño or La Niña precipitation pattern adequately. Recent model simulations [*Smith and Livezey*, 1999; *Livezey and Smith*, 1999] have demonstrated that predicting the ENSO signature on temperature in the United States improved dramatically once the long-term temperature trend was introduced in the model. Along the same lines we suggest that monitoring and incorporating into the prediction schemes the spatiotemporal trends of the precipitation field may provide an additional tool to improve the prediction of regional ENSO/precipitation patterns. Given the complex character of the precipitation field, it would be interesting to speculate on what factors might be involved in shaping up these trends. One may argue that while variable in sign, the signal observed in figures like Plate 3 is largely (though not exclusively) confined to the eastern United States. This may suggest that the North Atlantic/Arctic Oscillation and or the Pacific Oscillation may be playing a role. Work in this area is in progress, and the results will be reported elsewhere in the future.

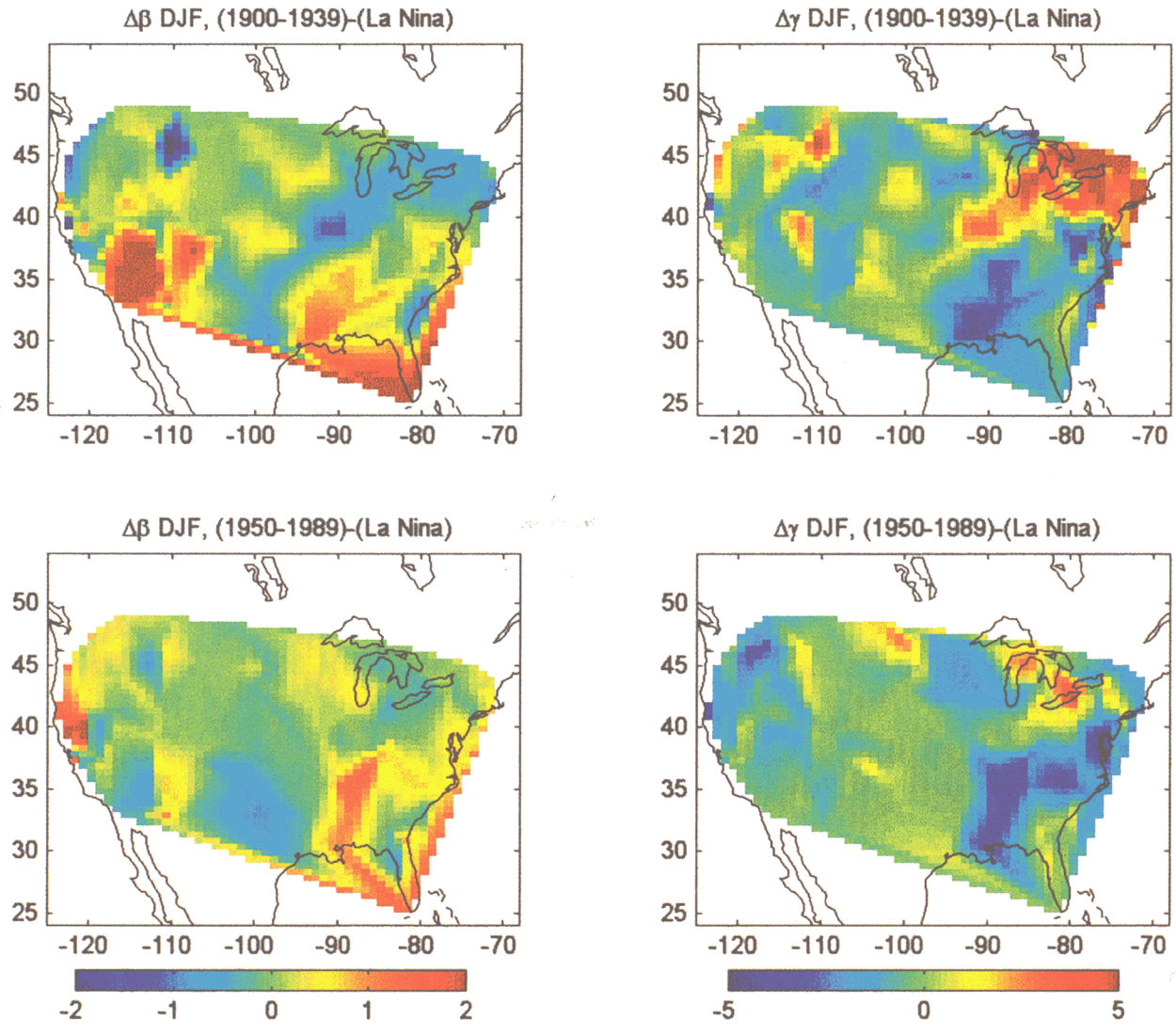

Plate 6. Same as Plate 5, but here the difference in (left) $\widehat{\beta}$ and (right) $\widehat{\gamma}$ is between selected 40-year intervals and the La Niña data set.

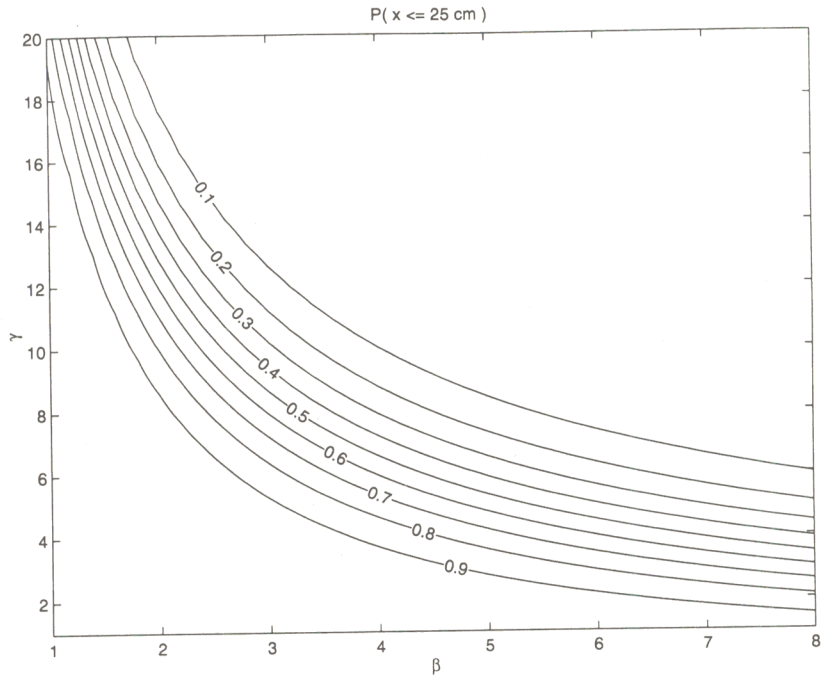

Figure 2. Probability that the DJF total precipitation amount will be less than or equal to 25 cm as a function of parameters β and γ of the gamma distribution. As it is explained in the text, great differences in that probability can be observed even for moderate changes in β and γ.

Acknowledgments. We like to thank Chet Ropelewski and two anonymous reviewers for their constructive comments. This work was supported by NOAA grant NA86GP0455.

References

Bradley, R. S., et al., Precipitation fluctuations over Northern Hemisphere land areas since the mid-19th century, *Science, 237,* 171-175, 1987.

Diaz, H. F., R. S. Bradley, and J. K. Eischeid, Precipitation fluctuations over global land areas since the late 1800s, *J. Geophys. Res., 94,* 1195-1210, 1989.

Gershunov, A., and T. P. Barnett, ENSO influence on intraseasonal extreme rainfall and temperature frequencies in the contiguous United States: Observations and model results, *J. Clim., 11,* 1575-1586, 1998a.

Gershunov, A., and T. P. Barnett, Interdecadal modulation of ENSO teleconnections, *Bull. Am. Meteorol. Soc., 79,* 2715-2725, 1998b.

Gershunov, A., T. P. Barnett, and D. R. Cayan, North Pacific interdecadal oscillation seen as a factor in ENSO-related North American climate anomalies (abstract), *Eos. Trans. AGU, 80,* 25 1999.

Karl, T. R., R. W. Knight, and N. Plummer, Trends in high-frequency climate variability in the twentieth century, *Nature, 377,* 217-220, 1995.

Livezey, R. E., and T. M. Smith, Covariability of aspects of North American climate with global sea surface temperatures on interannual to interdecadal timescales, *J. Clim., 12,* 289-302, 1999.

Ropelewski, C. F., and M. S. Halpert, Quantifying Southern Oscillation-precipitation relationships, *J. Clim., 9,* 1043-1059, 1996.

Ropelewski, C. F., and J. B. Jalickee, Estimating the significance of seasonal precipitation amounts using approximations of the inverse gamma function over an extended range, in *Proceedings of the 8th Conference on Probability and Statistics in Atmospheric Sciences,* pp. 125-129, Am. Meteorol. Soc., Boston, Mass., 1984.

Smith, T. M., and R. E. Livezey, GCM systematic error correction and specification of the seasonal mean Pacific-North America region atmosphere from global SSTs, *J. Clim., 12,* 273-288, 1999.

Thom, H. C. S., A note on the gamma distribution, *Mon. Weather Rev., 86,* 117-122, 1958.

Trenberth, K. E., et al., Progress during TOGA in understanding and modeling global teleconnections associated with tropical sea surface temperatures, *J. Geophys. Res., 103,* 14,291-14,324, 1998.

Tsonis, A. A., Widespread increases in low-frequency variability of precipitation over the past century, *Nature, 382,* 700-702, 1996.

A. A. Tsonis, Department of Mathematical Sciences, Atmospheric Sciences Group, University of Wisconsin-Milwaukee, Milwaukee, WI 53201-0413. (aatsonis@csd.uwm.edu.)

C. C. Young-Molling, Space Science and Engineering Center, University of Wisconsin-Madison, Madison, WI (ccmolling@facstaff.wisc.edu.)

(Received February 1, 2000 ; revised June 12, 2000 ; accepted September 20, 2000 .)